Effect of Above-Ground Oblique Impacts on the Performance of an Earth Penetrator

Introduction

Analyses of proposed impact scenarios suggest there is a reasonable probability that an earth penetrator will strike an obstacle before hitting the ground. Examples of potential obstacles include urban rubble (e.g., buildings and concrete slabs), boulders, and trees. Encounters with these obstructions could induce lateral impulses large enough to change the trajectory of the penetrator. Other workers have studied various aspects of this problem both analytically and experimentally. For example, Nelson et al.

To our knowledge, however, no closed-form solution based on first principles has been developed to treat problems of this type. Such a technique offers the advantage of simple implementation and rapid solution times compared to the computer-intensive numerical techniques that have been employed by other workers. Some of the computational methods that have been used include: CALSAP [2], an implicit finite element code; PROBS [2], an explicit time integration scheme; HULL, a 3-D finite element, Lagrangian/Eulerian, code [5]; and TRIFLE a quasi 3-D finite element code [6]. While these techniques provide useful solutions for a limited number of specialized problems, their complexity make it difficult to examine how these solutions might be affected by realistic parameter variations. For this reason, there is a need for a simplified, closed-form solution technique for problems of this type.

* Caliber is defined as the ratio of boulder diameter to penetrator diameter.

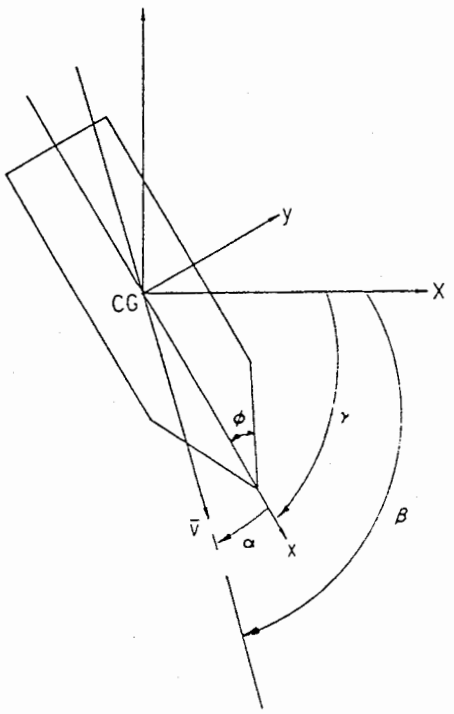

Figure 4. The Angle of Attack, α, Impact Angle, γ, Velocity Vector Angle, β, and the Nose Angle, ϕ.

and the time of contact between the penetrator and the boulder, t_{12}, is given by the EPW nose cone length, L_n, divided by the impact velocity.

The development of the equations of motion can be further simplified by assuming that the position of the boulder is fixed. That is, the boulder does not roll or slide under the action of F. This assumption can be readily justified for relatively massive boulders and high-velocity encounters. For example, a 4-foot diameter boulder would be expected to weigh on the order of 5500 lbs. This weight, plus the component of F acting in the Y-direction, along with a reasonable value for the static friction coefficient between the boulder and the ground will result in a large friction force, f_1, that will tend to prevent sliding of the boulder. In addition, for an impact velocity of 2000 fps, the time of contact between the boulder and the EPW will be on the order of 1 ms, which is too short a time for a 4-foot diameter boulder to respond as a rigid body. It is quite possible, of course, that a complete analysis of some other impact conditions will require an appropriate treatment of the boulder's motion. However, since it is expected that such analyses will be quite complex, they will be reserved for a separate, future study.

As a final simplification, we assume that the friction force between the EPW and the boulder, f_2, is zero. This assumption is justified by empirical studies indicating that the coefficient of sliding friction between a rock and a metal surface is on the order of 0.08 at high relative velocities [7].

It should also be noted that a special situation exists when the contact angle, θ, is less than $90 - \gamma + \phi$. When this condition occurs, the EPW's nose tip will not contact

the boulder. The contact area and the loading duration will be reduced, consequently reducing the lateral impulse. One scenario to illustrate this situation is given by an EPW with an initial impact angle of 90 degrees striking a spherical boulder as in Figure 5; the limiting contact angle would be ϕ, the nose cone angle (about 12 to 20 degrees). There is no such limitation for impacts with planar obstacles (e.g. a concrete slab).

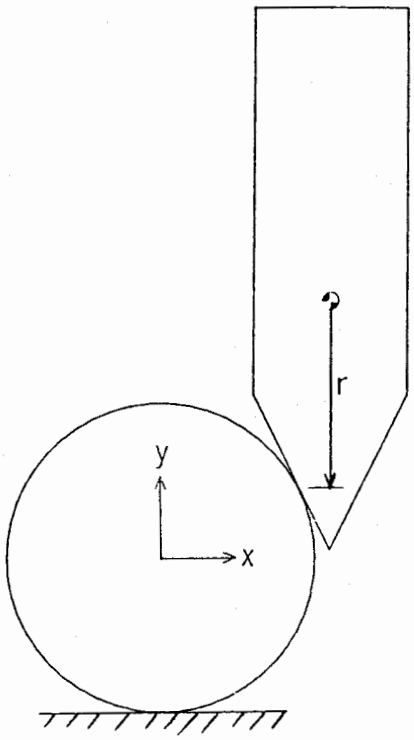

Figure 5. Effect of Reduced Moment Arm and Lateral Load Due to a Smaller Area of Contact.

2.2. Solving for the Impact Angle, γ

An expression for the final impact angle, γ_3, was derived first since it is independent of the other angles. The value of the impact angle at Point 2 can be computed by assuming the lateral impulse produces a constant angular acceleration:

$$\gamma_2 = \gamma_1 + \dot{\gamma}_1 t_{12} + \frac{1}{2}\ddot{\gamma}_{12} t_{12}^2, \tag{1}$$

where, in this case, positive γ is taken as counterclockwise, and

$$t_{12} = \frac{L_n}{v_1}, \tag{2}$$

$\dot{\gamma}_1$ is the first time derivative of the impact angle at Point 1, and $\ddot{\gamma}_{12}$ is the second derivative of the impact angle during time t_{12}. A similar equation can represent the change in γ from Point 2 to Point 3 where only gravity acts as a linear acceleration; furthermore, the angular velocity, $\dot{\gamma}_2$, is not zero. Thus an expression for γ_3 is given by:

$$\gamma_3 = \gamma_2 + \dot{\gamma}_2 t_{23} + \frac{1}{2}\ddot{\gamma}_{23} t_{23}^2 \tag{3}$$

where t_{23} is the time from Point 2 to Point 3, $\dot{\gamma}_2$ is the first time derivative of the impact angle at Point 2, and $\ddot{\gamma}_{23}$ is the second time derivative during the time t_{23} and is assumed to be zero since there are no external forces acting on the penetrator during this time. Substituting (1) into (2) we get

$$\gamma_3 = \gamma_1 + \dot{\gamma}_1 t_{12} + \frac{1}{2}\ddot{\gamma}_{12} t_{12}^2 + \dot{\gamma}_2 t_{23}. \tag{4}$$

The angular velocity, $\dot{\gamma}_2$, can be calculated at Point 2 from the equation

$$\dot{\gamma}_2 = \dot{\gamma}_1 + \ddot{\gamma}_{12} t_{12}. \tag{5}$$

We now solve for the angular acceleration from the moment equation, where F is a constant lateral force (assumed to act normal to the contacting tangential plane), and r is the distance from the tip of the penetrator's nose to its center of gravity. Thus:

$$\sum M_{cg} = \ddot{\gamma}_{12} I_{cg} \rightarrow \ddot{\gamma}_{12} = -\frac{Fr}{I_{cg}} \sin(\gamma_1 + \theta) \tag{6}$$

where I_{cg} is the pitch moment of inertia of the penetrator, and θ is the contact angle. We substitute (6) into (5), and subsequently substitute (5) into (4); This resolves into

$$\gamma_3 = \gamma_1 + \dot{\gamma}_1 \left[t_{23} + t_{12}\right] - \frac{Fr}{I_{cg}} \sin(\gamma_1 + \theta) \left[t_{12}^2 + t_{12} t_{23}\right]. \tag{7}$$

But t_{23} is still unknown; this can be solved from the quadratic equation which is derived from Newton's Second Law in the vertical direction. Thus:

$$t_{23}^2 - \frac{2}{g}\left[-v_1 \sin(\alpha_1 + \gamma_1) + \frac{F t_{12}}{M} \sin(\theta)\right] t_{23} - \frac{2}{g} y_2 = 0 \tag{8}$$

where M is the mass of the penetrator, and y_2 is the distance from Point 2 to the ground. If the gravity term is negligible after the projectile leaves the object, then

$$t_{23} = \frac{y_2}{v_1 \sin(\alpha_1 + \gamma_1) + F\frac{t_{12}}{M} \sin(\theta)}. \tag{9}$$

Using this equation for t_{23} for the EPW calculations amounted to less than 1% difference. y_2 is also unknown but can be evaluated from:

$$y_2 = H - v_1 \sin(\alpha_1 + \gamma_1) t_{12} - \frac{1}{2}\left[\ddot{y}_2 - \frac{F}{M} \sin(\theta)\right] t_{12}^2, \tag{10}$$

where

$$H = \frac{D}{2}\left[1 + \sin(\theta)\right] \tag{11}$$

in the case of a spherical boulder. The time rate of change in the unit vector of the velocity term is

$$\ddot{y}_2 = v_1(\dot{\gamma}_1 + \dot{\alpha}_1)\cos(\alpha_1 + \gamma_1). \tag{12}$$

Since $\dot{\gamma}_1$ and $\dot{\alpha}_1$ were assumed to be zero, $\ddot{y}_2$ is also zero. The change in the magnitude of the velocity results from the axial component of the force.

References

1. R. B. Nelson, Y. M. Ito, D. E. Burks, Y. Muki, J. A. Hollowell, and C. W. Miller, "Numerical Analysis of Projectile Penetration Into Boulder Screens," SL-83-11, U.S. Army Waterways Experiment Station, July 1983.

2. C. W. Miller, W. L. McKay, and J. A. Hollowell, "Penetration of $\frac{1}{7}$ Scale Model of a Semi–Armor Piercing (SAP) Bomb Into Confined Overlays: Test and Analysis," AVCO Systems Div., SL-83-19, U.S. Army Waterways Experiment Station, Sept. 1983.

3. Y. M. Ito, R. B. Nelson, and D. E. Burks, "Numerical Method for Rock Rubble Fortification Analysis," DNA 5869F, Cal Research and Tech., July 1981.

4. C. F. Austin, C. C. Halsey, and S. L. Berry, "Full–Scale Penetration Into Semi-confined Diorite Boulders by a Semi-Armor Piercing (SAP) Bomb and a Slendor Penetrator," NWCTP 6220, Naval Weapons Center, Sept. 1980.

5. D. A. Matuska and J.J. Osborn, HULL Documentation, VOL 1 (Technical Manual) and VOL 2 (Users Manual), Orlando Technology Report, Shalimar, Florida, 1987.

6. Y. M. Ito, R. B. Nelson, and F. W. Ross–Perry, "3–D Numerical Analyses of Earth Penetrator Dynamics," DNA 5404F, Defense Nuclear Agency, Jan 1979.

7. M. M. Hightower, private communication.

8. P. Yarrington, private communication.

9. M. L. Chiesa, private communication.